Methane ameliorates post-operative cognitive dysfunction by inhibiting microglia NF-κB/MAPKs pathway and promoting IL-10 expression in aged mice

Dan Zhang[a,b,c,1], Na Li[c,1], Yuanyuan Wang[a,b], Wenbin Lu[c], Yongyan Zhang[c], Yuanjie Chen[c], Xiaoming Deng[a,b,c,*,2], Xiya Yu[c,*,2]

[a] Jiangsu Province Key Laboratory of Anesthesiology, Xuzhou Medical College, Xuzhou 221004, Jiangsu, China
[b] Jiangsu Province Key Laboratory of Anesthesia and Anesthesia Application Technology, Xuzhou 221004, Jiangsu, China
[c] Faculty of Anesthesiology, Changhai Hospital, Second Military Medical University, Shanghai 200433, China

ARTICLE INFO

ABSTRACT

Postoperative cognitive dysfunction (POCD) is one of the most common complications after surgery. Accumulating evidence suggests that postoperative neuro-inflammation plays a critical role in the mechanism of POCD. Recently, exogenous methane is reported to have anti-inflammatory properties and play a neuro-protective role in acute carbon monoxide poisoning injury. Therefore, we investigated the protective effect of methane on a POCD model induced by abdominal surgery and its underlying mechanism in aged mice. Methane-rich saline (MS) or normal saline (NS) (16 ml/kg) was injected intraperitoneally 30 min after the abdominal surgery. The result showed that methane attenuated spatial memory loss in Morris water maze (MWM) with decreasing pro-inflammatory cytokines production and activation of microglia in hippocampus after surgery. Meanwhile, methane treatment suppressed lipopolysaccharide (LPS)-stimulated phosphorylation of MAPKs pathways and its downstream target TNF-α and IL-6 in BV2 cells. Moreover, methane increased expression of IL-10 in the hippocampus 24 h after surgery, and blockade of IL-10 repressed the protective effect of methane on the cognitive impairments observed in MWM test, decreased microglial activation and the pro-inflammatory cytokine in plasma and hippocampal. Blockade of IL-10 abrogated the suppression effect of methane on the pro-inflammatory cytokine production and phosphorylation of NF-κB and p38MAPK both in hippocampus and in BV2 cells. In conclusion, our study suggests exogenous methane could be a novel agent for the therapy of POCD through its anti-inflammation properties.

1. Introduction

Postoperative cognitive dysfunction (POCD) is defined by the deterioration in cognitive performance evaluated by neuropsychological tests before and after surgery [1]. As one of the most common long-term complications after surgery, POCD affects 30% of middle-aged and elderly patients during the first week after non-cardiac surgery in memory, learning, and attention capacity decline [2]. POCD adversely affects patient's post-operative perspective and brings significant clinical, social and financial impacts for patients' communities.

Methane, the most abundant organic gas compound on earth, used to be considered as biologically inactive [3]. Newly growing evidence suggests exogenous methane exerts protective effect in many ischemia-reperfusion injury models, including spine cord, liver, heart and intestine, which link to its redox regulation and attenuation of mitochondrial dysfunction [4–7]. Moreover, methane is shown to have beneficial effects on carbon monoxide poisoning encephalopathy, diabetic retinopathy, concanavalin A-induced autoimmune hepatitis, one-time exhaustive exercise capacity via anti-inflammatory, anti-oxidant or anti-apoptosis pathways [8–11]. Our recent work indicates that Methane-rich saline (MS) limits lipopolysaccharide-induced NF-κB and mitogen-activated protein kinase (MAPK) signaling in macrophages and suppresses innate immune responses in sepsis and DSS-induce colitis by enhancing anti-inflammatory cytokine IL-10 production [12]. However, whether methane plays protective role in cognitive dysfunction remains unknown.

* Corresponding authors at: Faculty of Anesthesiology, Changhai Hospital, The Second Military Medical University, 168, Changhai Road, Shanghai 200433, China.
E-mail addresses: deng_x@yahoo.com (X. Deng), yuxiyash@163.com (X. Yu).
[1] D.Z. and N.L. contributed equally to this work.
[2] X.M.D. and X.Y.Y. contributed equally to this work.

The innate immune system is the first line of the organism's defensive response to tissue damage or infection. More and more studies indicate that the innate immune response and neuro-inflammation have a crucial role in POCD [13]. Triggered by surgery and trauma, the integrity of the blood–brain barrier (BBB) is impaired by transient systemic immune response [14]. The activation of microglia, the primary immune cells of the central nervous system, plays a pivotal role in hippocampal neurogenesis and cognitive deficits. Thus, inhibition of the production of pro-inflammatory mediators would be a potential therapeutic strategy. Therefore, we investigate whether methane could prevent hippocampal neuro-inflammation and the impairment of neurological function induced by laparotomy surgery in aged mice. For the in vitro study, we examine whether methane can suppress lipopolysaccharide (LPS)-induced inflammatory mediators' production in cultured BV2 microglia cells and its underlying mechanisms.

2. Materials and methods

2.1. Animals

Male 24–25 months old C57BL/6 mice, were purchased from the Animals Experimentation Center of Second Military Medical University. All animals were kept pathogen free with a 12-h light/dark cycle and fed on a standard laboratory diet. Animal experiments were approved by the Committee on the Ethics of Animal Experiments of Second Military Medical University.

2.2. Methane-rich saline preparation

Previous studies indicated that [5,10] methane stored in gas canister was dissolved in normal saline under high pressure (0.4 MPa) for 3 h to a supersaturated level. Then, the saturated MS was stored under atmospheric pressure at 4 °C and freshly prepared one day before experiments in order to ensure the saturation concentration. Gas chromatography (Gas chromatography-9860, Qiyang Co, Shanghai, China) was implemented to disclose the content of methane in saline solute as previous study indicated. MS was supplied by the Department of Diving Medicine, Faculty of Navy Medicine, second Military Medical University (shanghai, china).

2.3. Administration of methane-rich saline

According to our previous studies [12], one dose of 16 ml/kg MS or saline were intra-peritoneal injected 30 min after surgery. The dose and timing of MS treatment in the dose-response study of BV2 cells was as indicated. For the in vitro experiments, BV2 cells were treated with MS (40 μl/ml) or saline at indicated time points after LPS stimulation.

2.4. POCD model

According to previous study [15], the laparotomy was set-up to mimic abdominal surgery in old patients. Mice were under general anesthesia (1.5% isoflurane in O_2 at 0.5 L/min) in an induction chamber. A 3 cm vertical incision was made and the viscera were explored. Then, the gastrointestinal tract was exteriorized. The small intestine were covered with a moist gauze, and then manipulated with a sterile cotton swab for 60 min. The body temperature was maintained at 37 °C with a heating lamp. The mice were divided into three groups randomly (25 mice per group): the control group received only general anesthesia (Ctrl), surgery group received a laparotomy with saline treatment (Surgery), and methane treatment group received a laparotomy with methane-rich saline (Surgery + MS). As for the anti-IL-10 antibody in vivo study, two more groups were added randomly (25 mice per group): isotype plus methane-rich saline group (Iso + Surgery + MS), and anti-IL-10 antibody plus methane-rich saline group (anti-IL-10 + Surgery + MS). All mice were administered buprenorphine

0.05 mg/kg subcutaneously for analgesia and returned to their home cages after the surgery.

2.5. Treatment with anti-IL10 antibody

Anti-IL10 antibody or isotype (ebioscience), suitable for in vivo blocking, was intraperitoneal injected 40 μg/per mouse 24 h before surgery. The dose of anti-IL-10 was chosen based on our previous study in a mouse model of systematic inflammation [12]. For BV2 cells, anti-IL10 antibody (5 μg/ml) or isotype was ~~intraperitoneally administrated~~ add 1 h before LPS stimulation [16].

2.6. Morris water maze

Morris water maze (MWM) testing was applied to assess spatial learning and spatial memory. Morris water maze task was performed in a round container (100 cm × 50 cm) (Jiliang Software, Shanghai, China) filled with water (21.5 ± 0.5 °C) containing food-grade titanium dioxide (Jianghu Taibai, Shanghai, China) in an isolated environment. Different shapes were marked on the inner walls of the pool for the orientation in the maze. The pool was divided into four quadrants and monitored with a video camera on the top. A platform (7 cm × 7 cm) was place 1 cm below the water surface in one of the four quadrants.

The MWM testing was started 3 days after the surgery to allow the abdominal wound to heal. All mice underwent 4 trials training daily. In each trial, mice were placed in water facing the wall of maze at one of four equally spaced entrance. Mice were allowed to search the platform and climb on it within 60 s. If the mice failed in 60 s, they would be guided onto the platform and allowed to stay on it for 10 s. The probe tests were performed with the platform removed after the trials. The training trial were performed for 5 continuous days. The escape latency, swimming time and speed spent in target quadrant were measured in a single 60-s trial. Average escape latency to the platform during training process was used as measure for spatial learning. In the probe trial, swimming speed and time in the target quadrant were used as measure for motor performance and spatial memory respectively.

On postoperative day 3 and day 7, working memory as tested after the probe trial. Both the platform and mice were randomly placed in novel positions for two trails [17]. Trail 1, the training session, was performed to ensure that all mice learned the new platform location. Trial 2 begins after a 15 s inter-trial interval. The mice would swim a shorter path to the platform in the Trial 2 if it recalled the Trial 1. The escape latency Trial 2 was taken as measure of working memory.

2.7. Cell culture

The BV2 cells (a mouse microglial cell line) were purchased from the Tongpai Biological Technology (Shanghai, China). The BV2 cells were cultured in DMEM supplemented with 10% fetal bovine serum (FBS) at 37 °C with 5% CO_2. Cells (1×10^5) were seeded into 24-well plates for cytokine assays, and 1×10^6 cells were seeded into 6-well plates for western blot analysis.

2.8. Cytokine measurement

The plasma and hippocampal tissue were collected at indicated time point after the POCD model. Since the activation of microglia play a pivotal role in hippocampal neurogenesis and cognitive deficits, BV2 cells stimulated by LPS were used as the POCD model in vitro. Supernatants from BV2 cells were collected 6 h after LPS stimulation. The level of TNF-α, IL-6 and IL-10 were detected by enzyme-linked immunosorbent assay (ELISA) kits (eBioscience, San Diego, CA) according to the manufacturer's instructions.
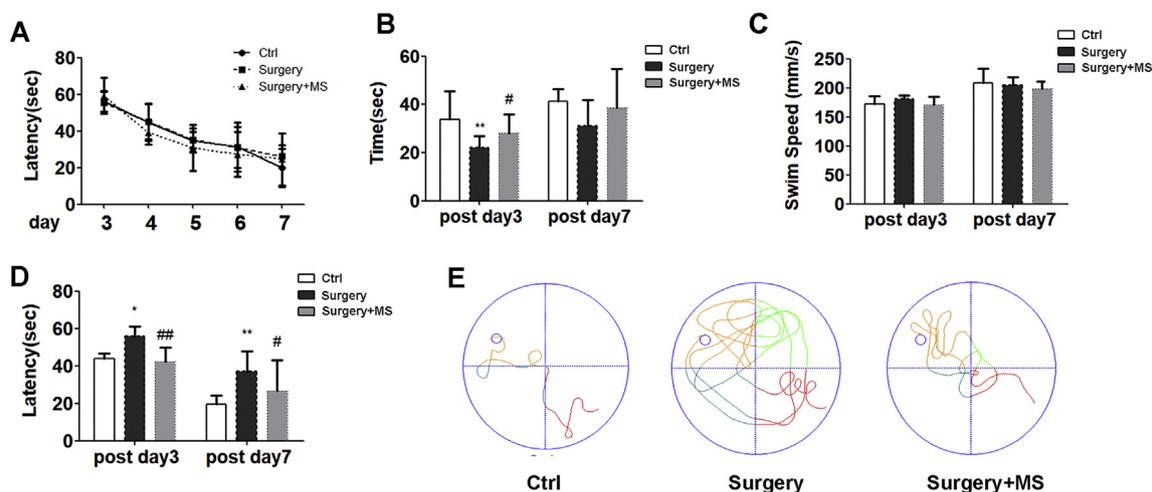
Fig. 1. Methane improve the impairment of behavioral performance induced by surgery in the aged mice. 3 days after surgery, mice were trained for consecutive five days. (A) Spatial learning in the MWM. Average escape latency (s) is shown for the five training sessions in the maze. On day 3 and day 7 post surgery, the time spent in the target quadrant (B) and swimming speed (C) were measured. The working memory trial was performed on day 3 and day 7 post surgery. Average escape latency (D) was recorded. (E) Representative swimming path of three groups on post Day 3 was shown. Data were expressed as mean $\pm$ SD ($n = 10$ per group). $^*P < 0.05$, $^{**}P < 0.01$, compared with Ctrl group, $^\#P < 0.05$, $^{\#\#}P < 0.01$, compared with Surgery group by two-way ANOVA test (A, B, C, D). Bars represent the mean $\pm$ SEM.

2.9. Real-time PCR

Mice were sacrificed at indicated time point after the model, and the mice hippocampal tissue were rapidly dissected and stored at $-80\,°C$. Total RNA was extracted with in Trizol reagent (Takara, DALIAN). Single strand cDNA was reverse-transcribed using a Prime Script RT Reagent Kit (Takara). The relative gene expression ofIL-6, TNF-α and IL-10 is calculated using $2^{-\Delta\Delta Ct}$ method. The murine primers were synthesized as follows:

IL-6:F5′-TACCACTCCCAACAGACCTG-3′
R5′-GGTACTCCAGAAGACCAGAGG-3′
TNF-α: F5′-AATGGCCTCCCTCTCATCAG-3′
R5′-CCCTTGAAGAGAACCTGGGA-3′
IL-10: F 5′-TGCCACTCAGAAGACTGTGG-3′
R5′-GTCCTCAGTGTAGCCCAGGA-3′
GAPDH: F5′-ATGGTGAAGGTCGGTGTGAA-3′
R5′-TGGAAGATGGTGATGGGCTT-3′

The mRNA levels were expressed as fold-changes after normalization to the reference gene GAPDH.

2.10. Western blot analysis

Western blot was performed according to standard methods. Briefly, BV2 cells were harvested at particular time points, the protein were isolated from cells in protein lysis buffer with protease inhibitor. Equal by the BCA protein assay kit (Thermo Fisher Scientific, Waltham, MA, USA), sample protein were loaded and separated by 10% sodium dodecyl sulfate-polyacrylamide gels (Life Technologies, Carlsbad, CA, USA) and transferred to nitrocellulose membranes (Life Technologies). Membranes were blocked for 1 h in 5% skim milk and then incubated overnight at 4 °C with primary antibodies: p65/p-p65, p38/p-p38, ERK/ P-ERK, JNK/p-JNK, GSK3β, GAPDH, actin(Signal Technology). The protein bands were demonstrated by an enhanced chemiluminescence (ECL) western blot kit (Thermo Fisher Scientific, Waltham, MA, USA). Band intensity was quantified using the Image J software and the protein expression was normalized to GAPDH/actin signals.

2.11. Immunohistochemistry

The mice were euthanized 24 h after operation under deep anesthesia and perfused with ice-cold saline and 4% paraformaldehyde. The brains were harvested from the mice and then post fixed overnight. Dehydrated with 30% sucrose in 0.01 M PBS, deeply frozen, brains were cut coronally in 10-μm-thick sections. And applied with 1:8000 rabbit-anti-ionized-binding adaptor protein IBA-1 (ab178847; Abcam). The IHC detection were finished by incubating sections for 2 h at room temperature with avidin-biotin peroxidase complex (Vectastain ABC kit, Vector, Burlingame, PA) and 0.075 mg/ml 3.3-diaminobenzidine (DAB) as a chromagen (color changing reagent), with hematoxylin counterstaining. All dilutions were made in 0.01 M PBS. All sections were thoroughly rinsed with 0.01 M PBS between staining steps.

Staining was analyzed in a blinded fashion in three sections per area for each animal. With the use of image analysis software (Image-J, 1.48v), the average total cell coverage, average cell body coverage of the IBA-1-positive cells in the hippocampus were determined. The cell body-to-total cell size ratio was used as a measure of microglia activation [18,19].

2.12. Statistical analysis

Data regarding biochemistry changes were expressed as mean $\pm$ standard deviation (SD). Data regarding Morris water maze test data were expressed as mean $\pm$ SEM. The number of samples varied from 6 to 10.The escape latency during the water maze training were compared using the two-way ANOVA test with Bonferroni's correction. The other comparisons among four groups were performed by the one-way ANOVA test, followed by Newman-Keuls test. All statistical analyses were performed using the GraphPad Prism 5.0 software (La Jolla, USA). $P < 0.05$ was considered statistically significant.

3. Results

3.1. Methane improved the memory impairment after surgery in the MWM test

According to the method reported by Zhang et al. [20], the protective effects of methane were examined in laparotomy surgery in aged rodents. The learning and memory ability of the mice was tested using the Morris water maze. As shown in Fig. 1A, the escape latency showed no difference between the groups. The latency was significantly shorter on the 5th day of training when compared to 1st day in all groups, indicating that all animals show equivalent spatial learning. In the

probe trail (Fig. 1B), the time spend in the target quadrant of Surgery group was significantly less than that of the Ctrl group on postoperative day 3. Methane treated group presented a longer time in the target quadrant, compared with the Surgery group, though still shorter than the Ctrl group. On postoperative day 7, there was no statistical difference between the Surgery group and other groups in dwelling time in the target quadrant. The swimming speed in the target quadrant (Fig. 1C) was similar among the three groups on postoperative day 3 and day 7, suggesting that the performance difference between groups was not a result of reduced motor ability. On postoperative day 3 and day 7, the working memory trial was performed (Fig. 1D). The latency time of Surgery group was significantly longer, comparing to the Ctrl group. Methane treated group significantly showed significantly shorter latency to board the platform, suggesting significantly improved cognitive function. Fig. 1E showed representative swimming path of the three groups on day 3 postoperative in the probe trial.

3.2. Methane treatment reduced systemic and hippocampus level of pro-inflammatory cytokines and decreased Iba-1-positive cells activation in hippocampus

Following the surgery, the levels of TNF- α and IL-6 in the plasma and hippocampus were measured at indicated time point. The systemic TNF-α and IL-6 concentration increase significantly after surgery, with the peak at 3 h. While methane application reduced the TNF-α and IL-6 cytokine expression level (Fig. 2A, Fig. 2B). In the hippocampus, TNF-α
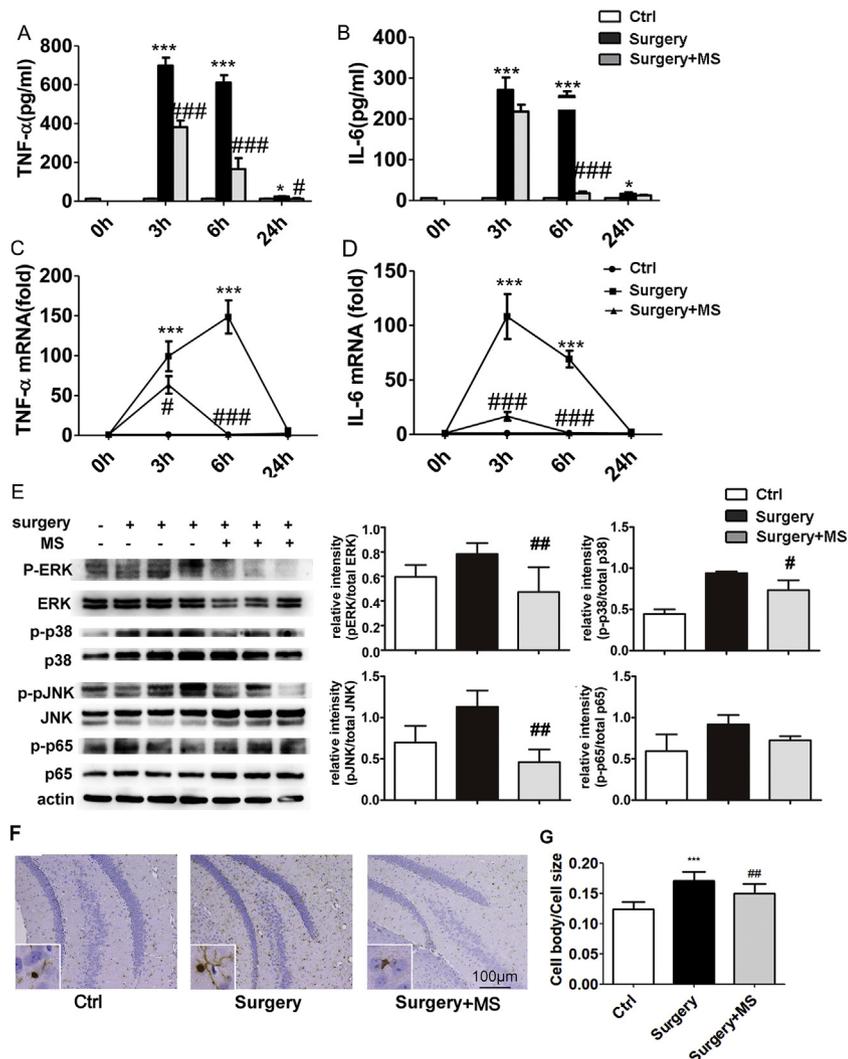
and IL-6 transcription levels of the Surgery group also elevated dramatically, compared with the Ctrl group, while significantly decreased by the treatment with methane (Fig. 2C, Fig. 2D). Also, we investigated methane's effect on the phosphorylation of NF-κB and MAPKs in the hippocampus 24 h after surgery (Fig. 2E). We observed phosphorylation of ERK, JNK, P38 and P65 in surgery group, while methane treatment significantly inhibited it. Surgery group were associated with a more elongated shape of the microglial cell bodies in the hippocampus and IBA1 is considered as the marker of microglial. We found methane treatment led to a decreasing activated level of IBA1-positive cells (Fig. 2F). The cell body-to-cell size ratio was used as measurement for microglia activation. The cell body-to-cell size ratio of Surgery group was increased in comparison with Ctrl group, while methane significantly reduces it.

3.3. Methane suppressed the activation of NF-κB and p38MAPK in LPS-activated BV2 cell

As shown in Fig. 3A–D, LPS stimulation significantly increased expressions of IL-6 and TNF-α in BV2 cells. To investigate the effect of methane on LPS-induced cytokine production, BV2 cells were treated with MS 30 min after LPS (100 ng/ml) stimulation for 6 h. MS significantly inhibited the pro-inflammatory cytokines (IL-6, TNF-α) production of in a dose-dependent manner (10, 20, 50 μg/ml). Furthermore, we investigated its effect on toll-like receptor(TLR)-induced phosphorylation of NF-κB and MAPKs in LPS-induced BV2 cells in vitro,

Fig. 2. Methane suppress pro-inflammatory cytokine in plasma and hippocampus as well as decrease IBA-1-positive cell activation in hippocampus induced by surgery. (A-B) The pro-inflammatory cytokines level of the serum was assessed by ELISA at indicated time point after surgery plus LPS. (C-D).MS post-treatment significantly decreased the production of IL-6 and TNF-α, especially 6 h after surgery. (E) Representative gel images and summary data show the MAPKs phosphorylation levels in the hippocampus 24 h after surgery. (F) Immunohistochemistry staining was used to detect IBA1-postive cells. Representative images of Iba1-labelled microglia in the hippocampus 24 h after surgery. Scale bar = 100 μm. (G) Microglia cell body-to-cell size ratio as measure for microglia activation in hippocampus. Results were presented as mean ± SD (n = 7 per group). * P < 0.05, ** P < 0.01, *** P < 0.001 compared with Ctrl group, # P < 0.05, ## P < 0.01, ### P < 0.001 compared with surgery group by two-way ANOVA test and Bonferroni's correction (A-F) or by one-way ANOVA and Newman-Keulstests (G). Bars represent the mean ± SD.
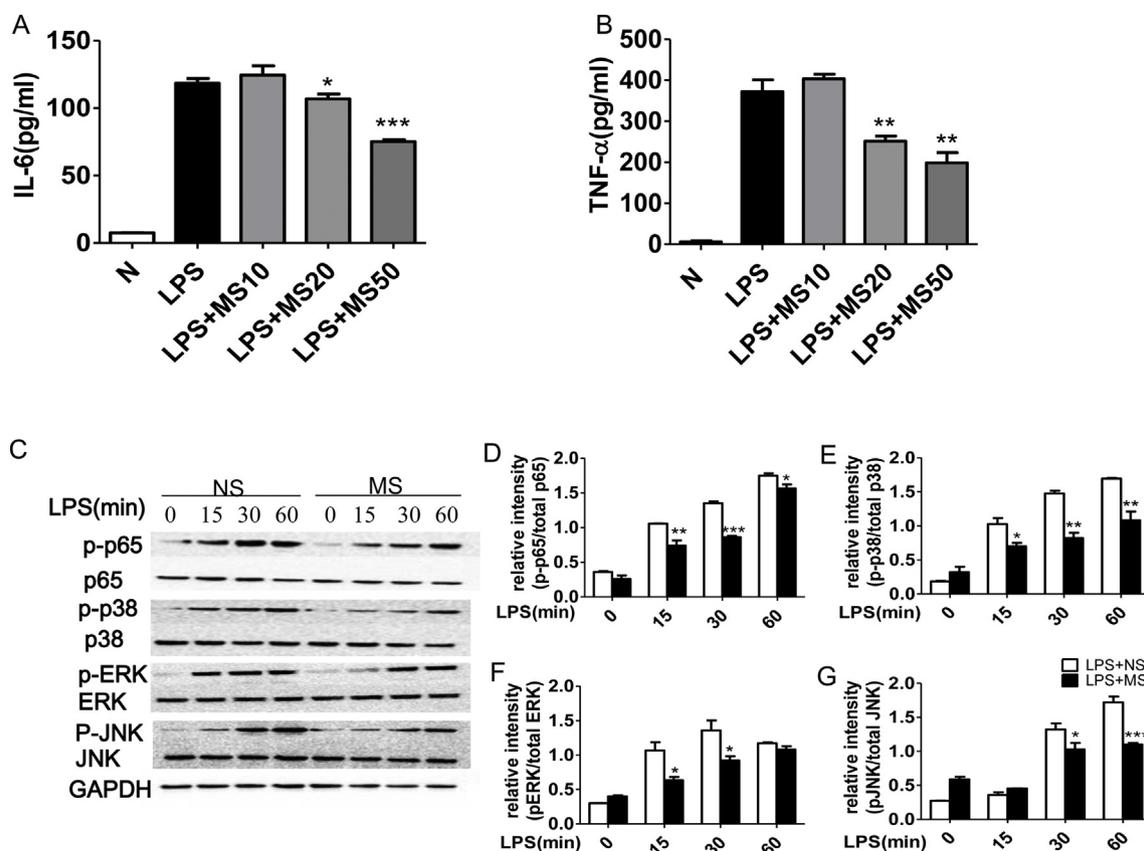
Fig. 3. MS post-treatment suppressed phosphorylation of NF-κB and MAPKs. (A-B)BV2 cells were stimulated with LPS (100 ng/ml) for 6 h, MS was added 30 min after LPS treatment at indicated concentrations (10, 20, 50 μg/ml). The supernatant were test by ELISA. BV2 cells were stimulated by 100 ng/ml LPS for different time, MS (40 μl/ml) or NS was added 5 min after LPS treatment, and western blotting was used to examine the indicated molecules. Representative gel images (C) and summary data (D-G) show the MAPKs phosphorylation levels in the BV2 cells at indicated time. Results were presented as mean ± SD. * $P < 0.05$, ** $P < 0.01$, *** $P < 0.001$ compared with LPS + NS group by one-way ANOVA and Newman-Keuls tests (A, B) or two-way ANOVA and Bonferroni's correction (D-G). Bars represent the mean ± SD.

which is widely used as a model for neuro-inflammation [21]. Our results showed that LPS stimulation caused a marked phosphorylation of ERK, JNK, P38 and P65. While methane treatment significantly inhibited it (Fig. 3C-G). Our Western blotting analyses demonstrated that MS could decrease the production of the pro-inflammatory cytokines via suppressing the activation of NF-κB and MAPKs of BV2 cells.
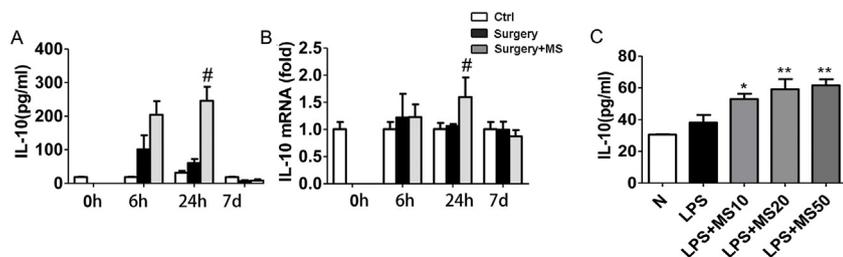
3.4. Methane treatment increase the expression of IL-10 in vivo and in vitro

IL-10, an anti-inflammatory cytokine, has pivotal roles in maintaining the balance of inflammatory response. It can down-regulate pro-inflammatory response and prevent tissue injury [22,23]. To investigate the possible anti-inflammatory mechanism of MS, we assessed IL-10 expression in plasma and hippocampal 6 h, 24 h and 7 day after surgery, and found that MS post-treatment mice exhibited higher level of IL-10 compared with Surgery + NS group, especially 24 h after surgery both in

plasma (Fig. 4A) and in the hippocampus (Fig. 4B). Meanwhile, methane treatment also increased the IL-10 production in BV2 cells 6 h after LPS stimulation (Fig. 4C).

3.5. The cognitive function protecting effect of methane in surgery could be rescued by IL-10 blockade

Anti-IL-10 antibody was given to aged mice to investigate whether IL-10 account for the improvement of the cognition impairment after surgery. In the working memory test (Fig. 5A), anti-IL10 reversed the shortened latency time of methane treated mice on postoperative day 3 and day 7. Also, in probe trial (Fig. 5B), Iso + Surgery + MS group spent more amount of time in the target quadrant than the anti-IL10 + Surgery + MS group on postoperative day. On postoperative day 7, there was no statistical difference between the all groups in dwelling time in the target quadrant. The distance travelled (Fig. 5C) was similar among

Fig. 4. Methane treatment increased the expression of IL-10 in vivo and in vitro. After surgery, blood and hippocampus of mice were collected at indicated time point. (A) Plasma level of IL-10 was determined by ELISA. (B) The mRNA of IL-10 in hippocampus was measured by quantitative real-time PCR. ($n = 7$ per group). (C) Level of IL-10 in BV2 cell supernatant 6 h after LPS stimulation with the post-treatment of NS or indicated dose of MS by ELISA. # $P < 0.05$ compared with surgery group by two-way ANOVA and Bonferroni's correction. * $P < 0.05$, ** $P < 0.01$ compared with LPS group by one-way ANOVA and Newman-Keuls tests. Bars represent the mean ± SD.
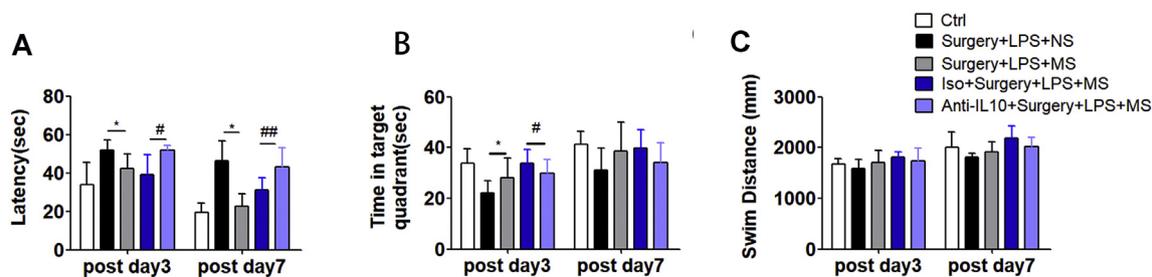
Fig. 5. The IL-10 blockade restored the protective effect of methane on spatial memory loss induced by surgery. Anti-IL10 antibody or isotype was intraperitoneal injected 40 μg/per mouse 24 h before surgery in the presence of MS or NS. (n = 6 per group) (A) Spatial learning in the MWM. Average escape latency is shown for the five training sessions in the maze. (B) Dwelling time in the target quadrant in the MWM probe trial on day 3 and day 7 after surgery. (C) Swimming distance in in the MWM probe trial on day 3 and day 7 after surgery. *$P < 0.05$ compared with surgery group, # $P < 0.05$ compared with Iso + surgery group, by two-way ANOVA test and Bonferroni's correction (A) or one-way ANOVA and Newman-Keuls test (B,C). Bars represent the mean ± SEM.

the four groups on postoperative day 3 and day 7, suggesting that the performance difference between groups was not a result of reduced motor ability.

3.6. IL-10A blockade increased microglial activation and the pro-inflammatory cytokine in plasma and hippocampal in methane treated mice after surgery

To investigate whether IL-10 plays the protective effect in POCD, anti-IL-10 antibody or isotype antibody was injected 24 h before the establishment of model. As shown in Fig. 6, anti-IL10 antibody application nearly completely abrogated the protective effect of MS, resulting in the upregulated activation IBA1-positive cells (Fig. 6A–B) as well as upregulating of IL-6 (Fig. 6C–E) and TNF-α (Fig. 6D–F) both at protein and mRNA level compared with the isotype group. Moreover, anti-IL10 antibody reversed the phosphorylation of ERK, and P38 of hippocampal in methane treated surgery group. While the GSK3β expression remained unchanged. These evidences suggested that IL-10 is required for the protective effect of MS in the surgery mice model and phosphorylation of ERK, and P38.MAPK may be involved in its mechanism.

3.7. IL-10A blockade abrogated the suppression effect of methane on the pro-inflammatory cytokine production and phosphorylation of NF-κB and p38MAPK in BV2 cells

To investigate whether the elevated IL-10 was necessary for anti-inflammatory effect of MS in BV2 cells, we analyzed TNF-α and IL-6 levels of LPS-stimulated BV2 cells in the presence of anti-IL10 antibody. As shown in Fig. 7A-B, the amount of TNF-α and IL-6 were restored in the presence of anti-IL10 antibody. Next, we investigate whether this reduced activation of NF-κB and p38MAPK also depend on the production of IL-10. Anti-IL10 antibody reversed the suppression effects of MS on phosphorylation of NF-κB and p38 MAPK (Fig. 7C-G). Moreover, such reversal effect was obvious in p65 and p38. These evidences showed that IL-10 may contribute to the suppression of NF-κB and p38MAPK pathway in BV2 cells caused by methane, which lead to decreased production of pro-inflammatory cytokine.

4. Discussion

This paper shows that abdominal surgery induced POCD in aged mice can be treated by methane. The protective effects of methane on the development of POCD in mice may be related to its anti-inflammatory effects, inhibiting microglial activation with MAPKs signaling and pro-inflammatory cytokines production down-regulation. Further, we found that blockade of IL-10 abolished the attenuation of memory function in methane-treated mice, activation of hippocampal microglial, and the inhibition of MAPKs signaling and related

downstream pro-inflammatory cytokines in BV2 cells.

Methane is the most common bacterial metabolic product. Lately research show it can be produced by the human gut, in some non-microbial such as fungi, mitochondria from cultured plant cells, and mammalian cells [8,24]. Methane was previously considered inert or biologically inactive [3] and not utilized by humans. Nevertheless, in the late 1960s, studies proved that methane participated in biological metabolism on sheep [25]. Further study from Boros proved that exogenous methane also has anti-oxidative and anti-inflammatory effects [7]. It has been demonstrated that the effect of methane-rich-saline was the same as that observed using methane inhalation [5,8]. Methane, dissolved into saline, is portable, safer and easily administered, can be prepared for clinical use. As the simplest alkane, methane could penetrate the cell membrane [26], let alone the blood–brain barrier [8] or blood-spinal cord barrier [4], which make it a promising therapy for central nerve system disorders. In the current study, we firstly illustrated that methane plays a protective role in POCD mouse model.

Neuro-inflammation can induce impairment of CNS function. Due to the protection of blood–brain barrier, CNS environment exhibit low exposure to systemic toxins and reduced traffic of inflammatory cells and molecules from circulating. The integrity of the BBB can be disrupted by the aseptic trauma of surgery induced systemic inflammatory response or anesthesia during and after surgery. Also, pro-inflammatory cytokines alone could play important part in BBB permeability impairment and center nervous system inflammation. The peripheral administration of TNF-α receptor antagonist or intracisternal administration of an IL-6 receptor antagonist notably reduced the neuro-inflammation and attenuated the relative cognitive deficit [27,28].

Microglia are the major resident immune cells of the CNS and have a lineage similar to peripheral macrophages, expressing both PAMP (Pathogen-associated molecular patterns) and DAMPs (Damage-associated molecular patterns) receptors. Activated microglia can be both neuroprotective and neurotoxic. Suppression of microglial activity exacerbates brain damage in hypoxic ischemic injury models [29]. Whereas, activated microglia themselves can produce cytokines, resulting in amplified neuro-inflammatory response to deleterious cognitive consequences in several neurodegenerative diseases, including Alzheimer's and Parkinson's diseases [30,31]. Our study showed that aged mice undergoing surgery displayed an exacerbated inflammatory response, as revealed by the mild activated microglia in hippocampus, with more condensed, less ramified morphology (Fig. 2.E). Methane suppressed the activation of microglia and the production of pro-inflammatory cytokines in hippocampus and in BV2 cells, which may be the mechanism of the protective effect of methane on POCD.

IL-10 is critical for maintaining normal neuro-immune communication during inflammation [32,33]. It has been reported that lipopolysaccharide leads to an increased expression of IL-beta and cell death in the hippocampus, which can be reduced by IL-10 [34]. In our study, we also found that treatment with MS remarkably increased the
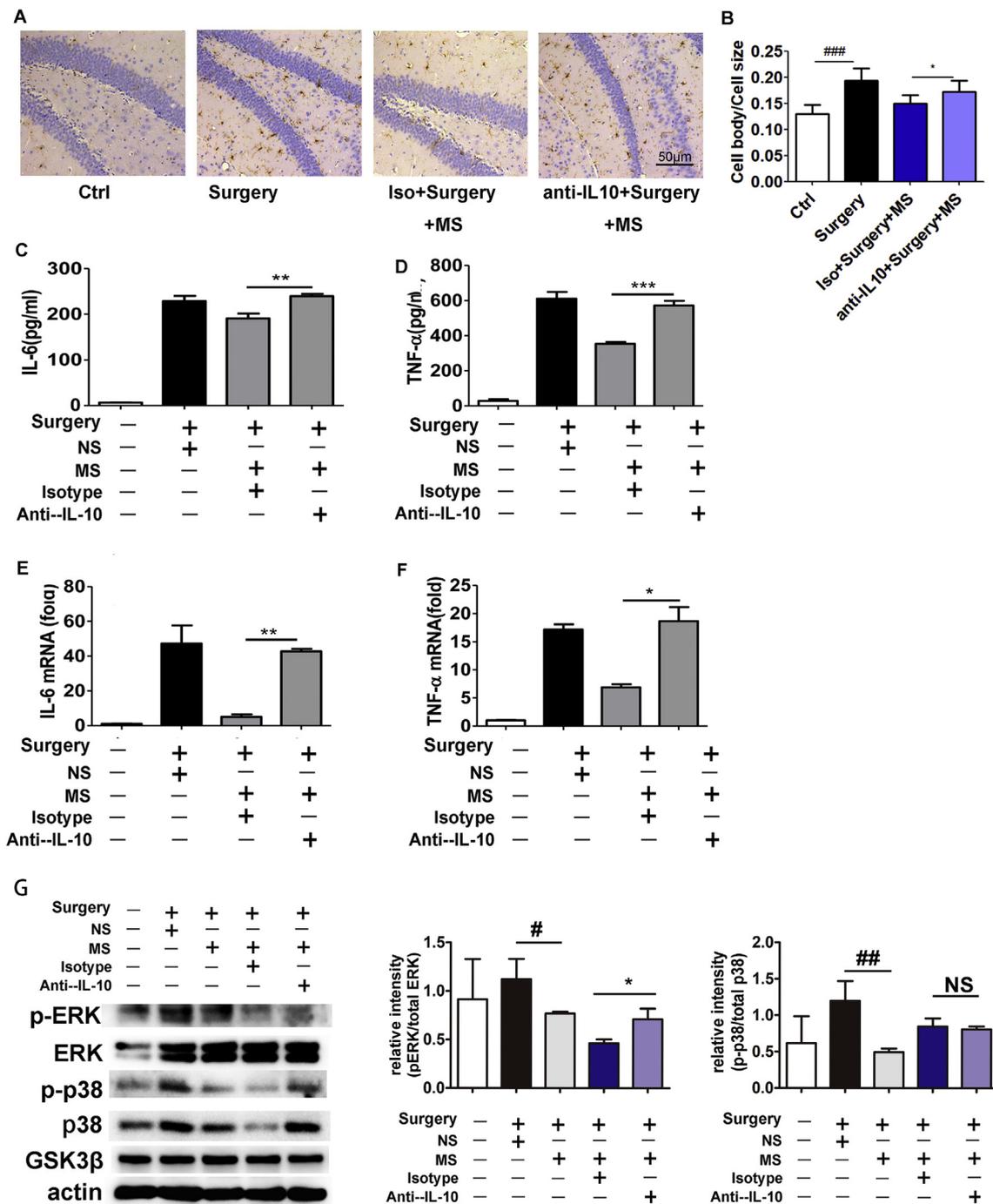
Fig. 6. The IL-10 blockade restored the methane improvement of spatial memory loss induced by surgery. Anti-IL10 antibody or isotype was intraperitoneal injected 40 μg/per mouse 24 h before surgery in the presence of MS or NS. (A) Representative images of Iba1-labelled activated microglia in the hippocampus 24 h after surgery. Scale bar = 50 μm. (B) Quantification of the activation of microglia in hippocampus zones by cell body/total cell size ratio. (C-D) 6 h post-surgery, blood sera and hippocampal tissues were collected. The production of IL-6 and TNF-α in plasma were analysis by ELISA. (E-F). TNFα and IL-6 mRNA level of hippocampal were measured by RT-PCR. (G) Representative gel images and summary data show the ERK and p38MAPKs phosphorylation levels and GSK3β level in the hippocampus 24 h after surgery. Results were presented as mean ± SD (n = 7, per group). *P < 0.05, ** P < 0.01, *** P < 0.001 compared with Iso + surgery group or # P < 0.05 compared with Ctrl group by one-way ANOVA and Newman-Keuls tests. Bars represent the mean ± SD.

expression of IL-10 in plasma and hippocampus of aged mice 6 h after establishment of POCD model. The beneficial effects of MS were inhibited through administration of anti-IL10 antibody, which is similar to the previous study demonstrating that the requirement of IL-10 in MS-mediated protective effect in TLR4-triggered immune response [12]. Meanwhile, blockade of IL-10 abrogate the MS-mediated improvement of cognition function as well as the decreased production of TNF-α and IL-6 in vivo.

In LPS-stimulated BV2 cells, anti-IL10 antibody reversed the MS-mediated decrease of TNF-α and IL-6 equally. Furthermore, the elevated level of IL-10 attenuated the LPS-induced activation of p65, p38, ERK and JNK both in hippocampus and in BV2 cells, which lead to the reduction on the level of TNF-α and IL-6. In brief, we believed that the IL-10 pathway may play important role in the protective effect of MS in POCD mouse model. Our date highlighted the comprehension of the anti-inflammatory mechanism of MS.
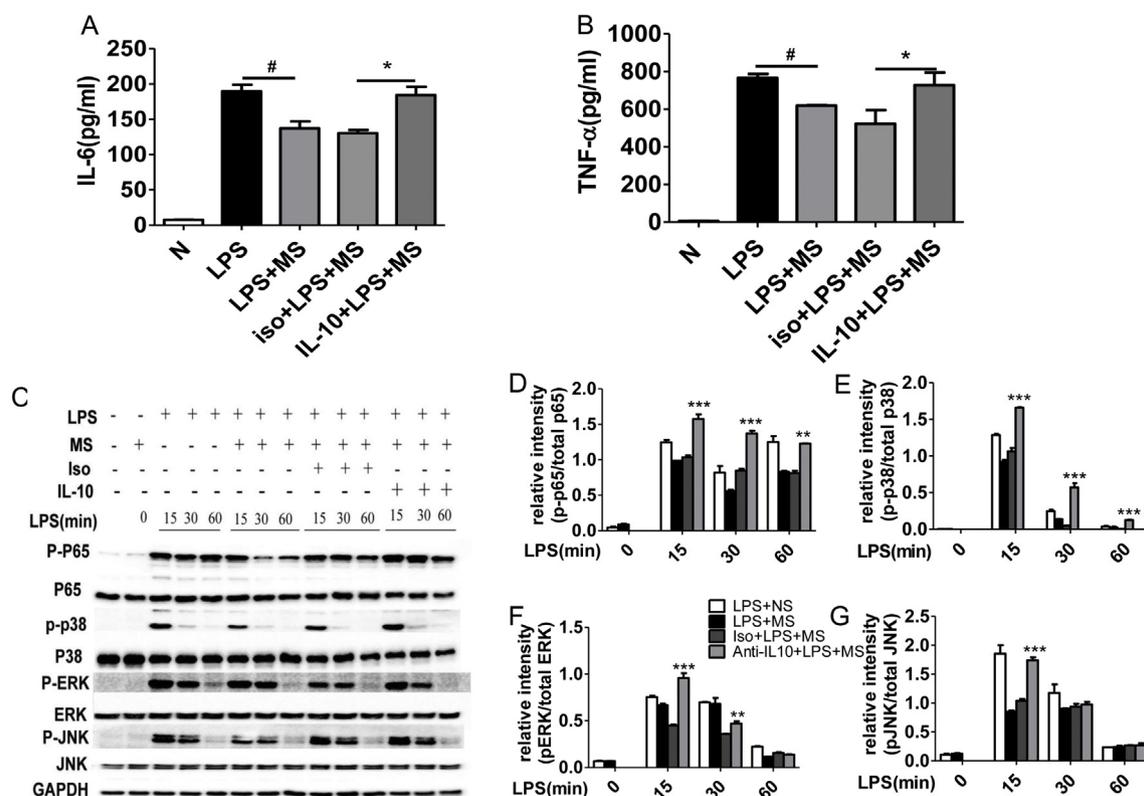
Fig. 7. Blockade of IL-10 reverses the attenuated activation of NF-κB and MAPKs in methane-treated BV2 cells. (A-B) BV2 cells were post-treated with 40 μl/ml MS and stimulated with 100 ng/ml LPS in the presence of 5 μg/ml isotype antibody or anti-IL-10 antibody. 6 h later, the supernatants were collected and the TNF-α and IL-6 levels were analyzed by ELISA. (C-G) BV2 cells were pre-treated with 5 μg/ml isotype antibody or anti-IL10 antibody for 1 h, followed by 100 ng/ml LPS. MS was added 5 min after LPS administration, and the phosphorylation of the MAPKs were examined at indicated time by western blotting (C). Results in C were quantified by determining the band intensity and calculated as phosphorylated signaling molecules to total corresponding molecules (D-G). Results were presented as mean ± SD. *P < 0.05, ** P < 0.01, *** P < 0.001 compared with LPS group or # P < 0.05 compared with Iso + LPS + MS group by one-way ANOVA and Newman-Keuls test.

Attention should be paid to the following limitations in our study. Firstly, we mainly focus on the protective role of methane on microglia. As mentioned above, BBB permeability dysfunction induces cognitive impairment following surgery [35]. Whether methane could act directly on brain microvascular endothelial cells, the main compartment of BBB, require more investigation. Secondly, the upstream pathway of IL-10 has not been thoroughly identified in our study. It has been proved that PI3K/AKT/GSK-3β pathway could mediate IL-10 expression induced by methane, whereas GSK-3β expression was unchanged in our animal model. Perhaps other signaling, like ERK and p38 MAPK [36] or CREB [37] may be involved. Finally, Besides IL-10 , IL-4 is also reported to act as negative regulator of activated microglia [38]. However, we did not found the elevation of IL-4 in hippocampus in MS treated mice (Fig. S). Whether other anti-inflammatory cytokines, like TGFβor IL-13, could be affected by methane treatment remains unclear. Further studies are urgently needed. In conclusion, our data suggest that methane-rich saline can reduce the neuro-inflammation induced by surgery plus LPS via promoting the production of IL-10 and inhibiting the activation of NF-κ B and P38MAPK in BV2 cells. Therefore this study illustrated that methane may be a promising target for the prevention and treatment of POCD.

Supplementary data to this article can be found online at https://doi.org/10.1016/j.intimp.2019.03.003.

Competing interests

The authors declare no competing financial interests.

Acknowledgements

References

[1] Berger M, Nadler J, Browndyke J, et al. Postoperative cognitive dysfunction: minding the gaps in our knowledge of a common postoperative complication in the elderly. Anesthesiol. Clin. 2015; 3: 517–550.
[2] Moller J T, Cluitmans P, Rasmussen L S, et al. Long-term postoperative cognitive dysfunction in the elderly ISPOCD1 study. ISPOCD investigators. International study of post-operative cognitive dysfunction. Lancet 1998; 9106: 857–861.
[3] Liu W, Wang D, Tao H, et al. Is methane a new therapeutic gas? Med. Gas Res. 2012; 1: 25.
[4] Wang L, Yao Y, He R, et al. Methane ameliorates spinal cord ischemia-reperfusion injury in rats: antioxidant, anti-inflammatory and anti-apoptotic activity mediated by Nrf2 activation. Free Radic. Biol. Med. 2017; 69–86.
[5] Ye Z, Chen O, Zhang R, et al. Methane attenuates hepatic ischemia/reperfusion injury in rats through antiapoptotic, anti-inflammatory, and antioxidative actions. Shock 2015; 2: 181–187.
[6] Chen O, Ye Z, Cao Z, et al. Methane attenuates myocardial ischemia injury in rats through anti-oxidative, anti-apoptotic and anti-inflammatory actions. Free Radic. Biol. Med. 2016; 1–11.
[7] Boros M, Ghyczy M, Erces D, et al. The anti-inflammatory effects of methane. Crit. Care Med. 2012; 4: 1269–1278.
[8] Fan D F, Hu H J, Sun Q, et al. Neuroprotective effects of exogenous methane in a rat model of acute carbon monoxide poisoning. Brain Res. 2016; 62–72.
[9] Wu J, Wang R, Ye Z, et al. Protective effects of methane-rich saline on diabetic retinopathy via anti-inflammation in a streptozotocin-induced diabetic rat model.

Biochem. Biophys. Res. Commun. 2015; 2: 155–161.

[10] He R, Wang L, Zhu J, et al. Methane-rich saline protects against concanavalin A-induced autoimmune hepatitis in mice through anti-inflammatory and anti-oxidative pathways. Biochem. Biophys. Res. Commun. 2016; 1: 22–28.

[11] L. Xin, X. Sun, S. Lou, Effects of methane-rich saline on the capability of one-time exhaustive exercise in male SD rats, PLoS One (3) (2016) e0150925.

[12] Zhang X, Li N, Shao H, et al. Methane limit LPS-induced NF-kappaB/MAPKs signal in macrophages and suppress immune response in mice by enhancing PI3K/AKT/GSK-3beta-mediated IL-10 expression. Sci. Rep. 2016; 29359.

[13] S. Saxena, M. Maze, Impact on the brain of the inflammatory response to surgery, Presse Med. 4 (Pt 2) (2018) e73–e81.

[14] Steinberg B E, Sundman E, Terrando N, et al. Neural control of inflammation: implications for perioperative and critical care. Anesthesiology 2016; 5: 1174–1189.

[15] Kawano T, Eguchi S, Iwata H, et al. Pregabalin can prevent, but not treat, cognitive dysfunction following abdominal surgery in aged rats. Life Sci. 2016; 211–219.

[16] Wu H Y, Tang X Q, Mao X F, et al. Autocrine Interleukin-10 mediates glucagon-like peptide-1 receptor-induced spinal microglial beta-endorphin expression. J. Neurosci. Off. J. Soc. Neurosci. 2017; 48: 11701–11714.

[17] C.V. Vorhees, M.T. Williams, Morris water maze: procedures for assessing spatial and related forms of learning and memory, Nat. Protoc. (2) (2006) 848–858.

[18] Fernandez-Arjona M D M, Grondona J M, Granados-Duran P, et al. Microglia morphological categorization in a rat model of neuroinflammation by hierarchical cluster and principal components analysis. Front. Cell. Neurosci. 2017; 235.

[19] I. Hovens, C. Nyakas, R. Schoemaker, A novel method for evaluating microglial activation using ionized calcium-binding adaptor protein-1 staining: cell body to cell size ratio, Neuroimmunol. Neuroinflam. 2 (2014) 82.

[20] Zhang Z, Li X, Li F, et al. Berberine alleviates postoperative cognitive dysfunction by suppressing neuroinflammation in aged mice. Int. Immunopharmacol. 2016; 426–433.

[21] Moniruzzaman M, Lee G, Bose S, et al. Antioxidant and anti-inflammatory activities of N-((3,4-Dihydro-2H-benzo[h]chromene-2-yl)methyl)-4-methoxyaniline in LPS-induced BV2 microglial cells. Biol. Pharm. Bull. 2015; 12: 1831–1835.

[22] Ouyang W, Rutz S, Crellin N K, et al. Regulation and functions of the IL-10 family of cytokines in inflammation and disease. Annu. Rev. Immunol. 2011; 71–109.

[23] S.K. Mittal, P.A. Roche, Suppression of antigen presentation by IL-10, Curr. Opin. Immunol. (2015) 22–27.

[24] Lenhart K, Bunge M, Ratering S, et al. Evidence for methane production by saprotrophic fungi. Nat. Commun. 2012; 1046.

[25] R.W. Dougherty, J.J. O'toole, M.J. Allison, Oxidation of intra-arterially administered carbon 14-labelled methane in sheep, Proceedings of the Society for Experimental Biology and Medicine Society for Experimental Biology and Medicine 4 (1967) 1155–1157.

[26] Pimentel M, Lin H C, Enayati P, et al. Methane, a gas produced by enteric bacteria, slows intestinal transit and augments small intestinal contractile activity. Am. J. Physiol. Gastrointest. Liver Physiol. 2006; 6: G1089–1095.

[27] Terrando N, Monaco C, Ma D, et al. Tumor necrosis factor-alpha triggers a cytokine cascade yielding postoperative cognitive decline. Proc. Natl. Acad. Sci. U. S. A. 2010; 47: 20518–20522.

[28] Jiang P, Ling Q, Liu H, et al. Intracisternal administration of an interleukin-6 receptor antagonist attenuates surgery-induced cognitive impairment by inhibition of neuroinflammatory responses in aged rats. Experimental and Therapeutic Medicine 2015; 3: 982–986.

[29] Faustino J V, Wang X, Johnson C E, et al. Microglial cells contribute to endogenous brain defenses after acute neonatal focal stroke. J. Neurosci. Off. J. Soc. Neurosci. 2011; 36: 12992–13001.

[30] Pena-Altamira E, Petralla S, Massenzio F, et al. Nutritional and pharmacological strategies to regulate microglial polarization in cognitive aging and Alzheimer's disease. Front. Aging Neurosci. 2017; 175.

[31] L. Qian, P.M. Flood, J.S. Hong, Neuroinflammation is a key player in Parkinson's disease and a prime target for therapy, Journal of Neural Transmission (Vienna, Austria: 1996) 8 (2010) 971–979.

[32] Tegeler C, O'sullivan J L, Bucholtz N, et al. The inflammatory markers CRP, IL-6, and IL-10 are associated with cognitive function–data from the Berlin Aging Study II. Neurobiol. Aging 2016; 112–117.

[33] Richwine A F, Sparkman N L, Dilger R N, et al. Cognitive deficits in interleukin-10-deficient mice after peripheral injection of lipopolysaccharide. Brain Behav. Immun. 2009; 6: 794–802.

[34] Lynch A M, Walsh C, Delaney A, et al. Lipopolysaccharide-induced increase in signalling in hippocampus is abrogated by IL-10–a role for IL-1 beta? J. Neurochem. 2004; 3: 635–646.

[35] Yang S, Gu C, Mandeville E T, et al. Anesthesia and surgery impair blood-brain barrier and cognitive function in mice. Front. Immunol. 2017; 902.

[36] Elcombe S E, Naqvi S, Van Den Bosch M W, et al. Dectin-1 regulates IL-10 production via a MSK1/2 and CREB dependent pathway and promotes the induction of regulatory macrophage markers. PLoS One 2013; 3: e60086.

[37] D.E. Sanin, C.T. Prendergast, A.P. Mountford, IL-10 production in macrophages is regulated by a TLR-driven CREB-mediated mechanism that is linked to genes involved in cell metabolism, J. Immunol. (3) (2015) 1218–1232.

[38] Fenn A M, Henry C J, Huang Y, et al. Lipopolysaccharide-induced interleukin (IL)-4 receptor-α expression and corresponding sensitivity to the M2 promoting effects of IL-4 are impaired in microglia of aged mice. Brain Behav. Immun. 2012; 5: 766–777.